https://ntrs.nasa.gov/search.jsp?R=20190000831 2020-05-09T15:46:59+00:00Z

TRAJECTORY ANALYSIS FOR THE HELIOCENTRIC PHASE OF THE DART MISSION

Bruno V. Sarli[a]
Catholic University of America, Washington D.C, 20064

Justin A. Atchison[2] and Martin T. Ozimek[2]
The Johns Hopkins University Applied Physics Laboratory, Laurel, MD, 20723

Jacob A. Englander[3] and Brent W. Barbee[3]
NASA Goddard Space Flight Center, Greenbelt, MD, 20771

DART, Double Asteroid Redirection Test, will be the first mission to demonstrate and characterize the concept of a kinetic impactor for planetary defense, by impacting the smaller member of a binary asteroid system Didymos. Results of this mission will have implications for planetary defense, Near-Earth Object science, and resource utilization. This research focuses on the heliocentric transfer phase of the mission. The heliocentric trajectory is evaluated using various objective functions, including a search for the latest possible escape date, the shortest time-of-flight, and the maximum impact energy. Also included in the search is the potential to use Earth gravitational assists, which proves not to offer any useful advantages. A new way to assess the trajectory's margin for missed thrust is used, which quantifies the ability of the spacecraft to recover its mission following unplanned non-thrusting events, such as safe-mode. The baseline trajectory is shown to be capable of recovering from missed thrust events lasting 14 days using only 1% of its propellant as margin. Finally, we consider contingency trajectories that attempt to impact Didymos at a subsequent perihelion.

[a] Associate Researcher, Physics Department, 620 Michigan Ave NE.
[b] Senior Professional Staff, Astrodynamics and Control Systems Group, 11100 Johns Hopkins Rd.
[c] Aerospace Engineer, Navigation and Mission Design Branch, 8800 Greenbelt Rd.

Nomenclature

(Nomenclature entries should have the units identified)

Δv	= instantaneous velocity change
ϕ_S	= solar phase angle
$\hat{\mathbf{r}}_{A/B}$	= generic position unit vector pointing from A to B
$\hat{\mathbf{v}}_{A/B}$	= generic velocity unit vector of A relative to B
ϕ_I	= impact angle
ϕ_{OP}	= out-of-plane component of the impact angle
ϕ_{IP}	= in-plane component of the impact angle
$\mathbf{h}_{OP}$	= generic orbital momentum vector vector of A relative to B
$\{\hat{\mathbf{x}}^I, \hat{\mathbf{y}}^I, \hat{\mathbf{z}}^I\}$	= x, y and z positions on the inertial coordinate system
$\{\hat{\mathbf{x}}^L, \hat{\mathbf{y}}^L, \hat{\mathbf{z}}^L\}$	= x, y and z positions on a generic local coordinate system
$A^{L/I}$	= rotation matrix from inertial to a local generic frame

I. Introduction

The Double Asteroid Redirection Test (DART) will be the first mission to demonstrate and characterize the concept of a kinetic impactor for planetary defense [4, 5]. Kinetic impactors are a class of planetary defense options where a spacecraft alters the orbit of a hazardous object by impacting it in advance. Upon impact, the spacecraft transfers linear momentum to the object, which is equivalent to a small and instantaneous change in velocity, Δv, that eventually results in the object missing Earth. This approach is most relevant for objects roughly smaller than a kilometer in diameter with tens of years of warning time [3]. These asteroid sizes are consistent with the relatively recent impacts of the Chelyabinsk [1] and Tunguska [2] meteors.

The DART spacecraft impacts the smaller member of a binary asteroid system (65803) Didymos, composed of the primary Didymos-A and secondary Didymos-B. By measuring the resulting change in the system's relative orbit period, Earth based observers can infer the efficacy of the impactor, including the so-called momentum enhancement factor. For the same imparted energy and momentum, the mutual binary orbit period change is more easily observed than the heliocentric period

change. In this case, a small spacecraft (∼500 kg) impacting at roughly 6 km/s can impart an orbit period change that is measurable from Earth-based observers within days or weeks. The results of this mission will have implications for planetary defense, Near-Earth Object science, and resource utilization. When launched, DART will represent a number of spaceflight firsts. First use of the NEXT ion propulsion system, first use of a commercial rideshare for interplanetary flight, and first interplanetary escape from GTO (considering that the SMART-1 mission was not interplanetary).

In addition to being the first planetary defense mission, it also serves as the first flight demonstration of the NASA Evolutionary Xenon Thruster (NEXT) [9], a gridded ion propulsion system. DART uses NEXT to escape Earth from an initial geostationary transfer orbit. NEXT is then used to fly by an asteroid (138971) 2001 CB_{21}, during which the spacecraft conducts a rehearsal of the terminal guidance phase. The asteroid (138971) 2001 CB_{21} was selected from a close approach scan on a reference trajectory that did not have it included. The objective was to deviate from the reference trajectory as little as possible. This intermediate flyby is strategic for the mission final operations because it allows sensor calibration and control-gain tuning prior to the impact. Finally, DART impacts its target Didymos-B, the secondary member of the Didymos system [6], using autonomous terminal guidance algorithms. The impact occurs during a rare conjunction of Earth and Didymos in October of 2022. During this conjunction, Didymos is below the ecliptic plane. As a result, much of DART's thrust profile is associated with achieving a target heliocentric inclination of roughly 3°.

DART went through a major change in its mission and system design; previous iterations of the spacecraft trajectory used hydrazine propellant only [5]. Following a trade-study [15], electric propulsion was selected because it offers key benefits to the DART mission. It reduces the mission cost, in that DART can launch as a secondary payload on another mission's Earth-bound orbit. Nominally, DART will launch on a geostationary transfer orbit associated with a U.S. government or commercial satellite launch. Electric propulsion also enables an asteroid flyby over any of the launch dates. This was not achievable with the chemical trajectory approach. Finally, electric propulsion allows the DART trajectory to be updated after launch, as new information about the Didymos system becomes available.

This mission design research focuses on the heliocentric transfer phase of the mission, including validation of the preliminary baseline trajectory, a performance comparison of mission objectives, and assessment of the trajectory with regards to missed thrust events. For the validation effort, two independent low-thrust optimization tools were used to determine the optimal trajectory subject to key mission constraints. This validation approach suggests that the resulting trajectory has agreement in terms of the underlying dynamics and is uniquely optimal. The objective function is then varied to assess different relevant mission metrics, including a search for the latest possible escape date, the shortest time-of-flight, and the maximum impact energy. Its resulting trajectories give context for the available DART trajectory trade-space. The baseline trajectory is assessed with respect to missed thrust events. That is, we quantify the ability of the spacecraft to recover its mission following unplanned non-thrusting cases, such as safe-mode. This is achieved using a new approach where the recoverable missed-thrust duration is explicitly maximized at each time-point within the trajectory. Although computationally expensive, this method gives a direct metric of trajectory robustness. Finally, we consider contingency trajectories that attempt to impact Didymos at a subsequent perihelion. A relevant study for cases where the spacecraft is unable to recover from a missed thrust event in sufficient time or the nominal impact is not completed successfully.

II. Methodology

The overall DART trajectory can be divided into three phases: Earth Escape Spiral, Heliocentric Transfer, and Terminal Impact. A summary of the baseline design for each of these phases is given in [14]. The Earth Escape Spiral incorporates critical subsystem requirements such as the programmatic launch period, the maximum eclipse duration, the maximum time in the radiation belts, and spacecraft attitude requirements. Roughly two thirds of the deterministic xenon propellant is used during this phase. The Heliocentric Transfer begins at the point of Earth escape, defined as the point at which the two-body orbital energy of DART is positive with respect to Earth ($C_3 > 0$). It includes the asteroid flyby and ends at 12 hours prior to impact when the Terminal Impact phase begins. During the Terminal Impact phase, the spacecraft uses on-board closed-loop guidance to target Didymos-B autonomously. This study focuses solely on the Heliocentric Transfer phase, which inherits its initial state from the Earth Escape Spiral phase and must satisfy final-state

constraints required by the Terminal Impact Phase.

A. Low Thrust Model

To Simplify the propulsion system architecture, the DART ion propulsion system (IPS) nominally operates at a constant setting, throttle Level 28, as specified in NEXT Throttle Table 11 [9]. Although DART's expected xenon consumption is modest compared to preflight testing, its performance is modeled with end-of-life values for conservatism. The baseline trajectory is designed using a 90% duty cycle, of which 5% is allocated as capability margin, i.e., thrust magnitude margin that can be used at any time to recover from anomalous deviation from the reference trajectory. Flight system configurations presented here were a result of detailed preliminary trade studies presented in reference [14]. Table 1 summarizes the IPS parameters used in this study.

Table 1 DART Spacecraft and Mission Characteristics

Earliest escape date (zero energy state)	Oct 03, 2021
Ion Engine Thrust	0.1371 N
Ion Engine Isp	3093 s
Duty-cycle	90%
Spacecraft Escape Mass	568.1 kg

B. Trajectory Constraints

The Heliocentric Transfer phase is propagated and optimized using a finite-burn low-thrust transcription that includes the gravity of the Earth and the Sun [11]. Every DART trajectory must satisfy the following constraints:

- **Continuity** - The initial state (time, position, velocity, mass) of the Heliocentric Transfer phase must match the final state of the Earth Escape Spiral phase identically. This satisfies a requirement that the DART trajectory be continuous from launch to impact.

- **Available Propellant** - The trajectory must not consume more xenon propellant than is available for the current system design. This constraint is also cast as an objective depending on the case under study.

- **Forced Coast** - Prior to the asteroid flyby and the impact, the trajectory must guarantee at least 30 days of coast. This period of ballistic flight facilitates optical navigation for these critical events.

- **Impact Date** - The impact experiment is timed to occur when Earth is within range to observe the event. This limits the time of impact to a window between September 25 and October 20 of 2022.

- **Arrival Solar Phase Angle** - DART's terminal guidance operates using images from an optical telescope with the Didymos target scene is illuminated by the Sun only. Lighting affects detection range as well as image-centroiding accuracy. In addition, the lighting conditions have implications on the ability to reconstruct the impact point using the final returned images. The solar phase angle, ϕ_S, is the angle connecting the instantaneous DART, Didymos-B, and Sun points. For mission success, the arrival solar phase angle is required to be less than or equal to 60°. Equation 1 outlines the computation of this term.

- **Arrival Impact Angle** - The DART impact experiment is measured by the imparted change in the Didymos system's mutual orbit period. This quantity is maximized if the impact occurs in a direction collinear with Didymos-B's relative orbit velocity. The impact angle, decomposed into an in-plane and out-of-plane component, is a means of ensuring that the experiment will result in a useful measurement. The definitions, equations, and bounds for these angles are given in the next sections. Impact momentum transfer models are not directly used in this study. Precise impact studies require detailed numerical analysis[17] for calculating the momentum transfer. Less precise determinations can be made using the conservation of linear momentum equation.

1. Arrival Constraints

The arrival solar phase angle and impact angle are defined here, as constructed for the trajectory optimization problem. Illustrating the impact geometry, Figure 1 uses correct scaling for the relative sizes of Didymos-A, Didymos-B, and the orbit radius. By using the unit vector pointing from

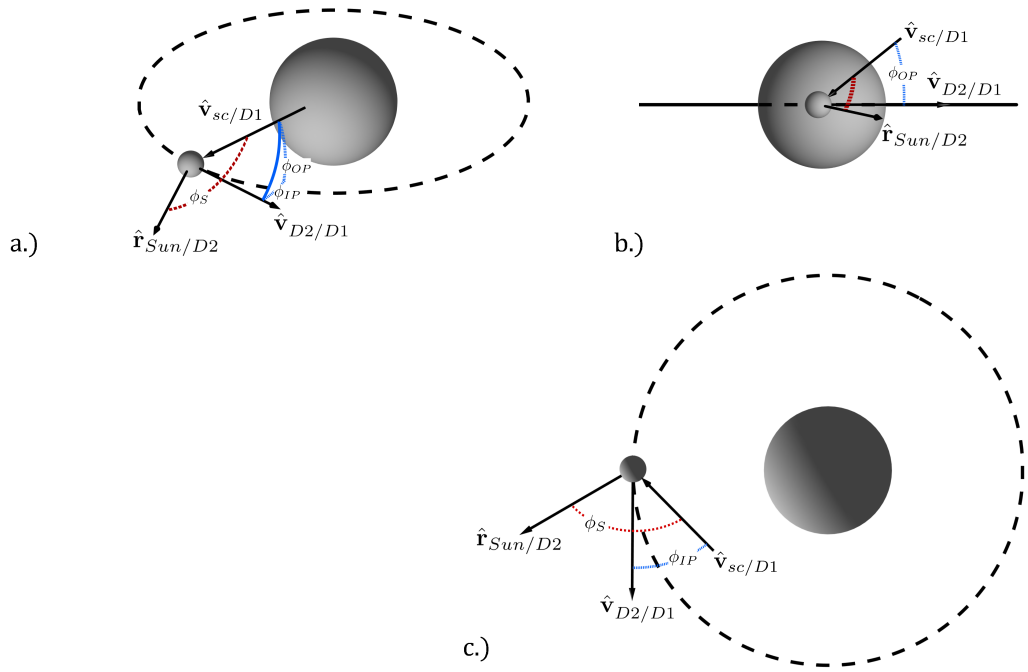

Fig. 1 Didymos arrival constraints depicted from three views: a.) perspective, b.) from within the mutual orbit plane, and c.) from along the mutual orbit normal.

Didymos-B to the Sun, $\hat{\mathbf{r}}_{\mathrm{Sun/D2}}$, and the unit vector associated with the velocity of the DART spacecraft relative to Didymos-B $\hat{\mathbf{v}}_{\mathrm{sc/D2}}$ one can compute the solar phase angle ϕ_{S}.

$$\phi_{\mathrm{S}} = \cos^{-1}\left(\hat{\mathbf{r}}_{\mathrm{Sun/D2}} \cdot -\hat{\mathbf{v}}_{\mathrm{sc/D2}}\right) \tag{1}$$

Similarly by using unit vectors, the impact angle ϕ_{I} can be defined as the angle between DART's velocity $\mathbf{v}_{\mathrm{sc/D1}}$ and Didymos-B's velocity relative to Didymos-A $\mathbf{v}_{\mathrm{D2/D1}}$.

$$\phi_{\mathrm{I}} = \cos^{-1}\left(\hat{\mathbf{v}}_{\mathrm{sc/D1}} \cdot \hat{\mathbf{v}}_{\mathrm{D2/D1}}\right) \tag{2}$$

This angle can be decomposed into two components, an in-plane angle and an out-of-plane angle. These are relevant because the momentum that is imparted out-of-plane changes Didymos-B's orbit plane, which is much less observable than in-plane changes to orbit period. To maximize the observability of the experiment, DART's arrival relative velocity must lie near to Didymos-B's orbit plane.

The out-of-plane component of the impact angle, ϕ_{OP}, is a signed angle that is required to have a value between $\pm$ 30°. The sign indicates the direction of the angle relative to Didymos-B's orbit momentum vector $\mathbf{h}_{\mathrm{D2/D1}}$. A value of +90° points opposite to $\mathbf{h}_{\mathrm{D2/D1}}$, 0° is in the Didymos-B mutual orbit plane, and −90° is directed along $\mathbf{h}_{\mathrm{D2/D1}}$.

$$\phi_{\mathrm{OP}} = \cos^{-1}\left(\hat{\mathbf{v}}_{\mathrm{sc/D1}} \cdot \hat{\mathbf{h}}_{\mathrm{D2/D1}}\right) - 90^\circ \tag{3}$$

The in-plane impact angle ϕ_{IP} is an unsigned angle that relates the orientation of the DART arrival velocity with Didymos-B's instantaneous velocity about Didymos-A, projected into the mutual orbit plane. Because Didymos-B's velocity relative to Didymos-A is changing with a period of roughly 11.9 hours, the in-plane impact angle is very sensitive to small (minute or hour) changes in arrival time. For an optimal impact, this angle will be either 0 or 180° in order to maximize the change in orbit period. For the current DART and Didymos system geometry, the desired angle is 180°, because this orientation places the impact on the sunward side of Didymos-A, which improves local lighting conditions.

Construction of a local coordinate system is required for computing ϕ_{IP}. This coordinate system is aligned with Didymos-B's orbit angular momentum ($\hat{\mathbf{z}}^M = \hat{\mathbf{h}}_{\mathrm{D2/D1}}$). The remaining orientation is constrained using an arbitrary reference vector. In this case, the inertial y axis is used ($\hat{\mathbf{y}}^I = [0 \quad 1 \quad 0]$). The superscript M denotes this mutual coordinate system and superscript I denotes the inertial coordinate system that the inputs are provided in.

$$\mathbf{Q}^{M/I} = \begin{bmatrix} \hat{\mathbf{x}}^M & \hat{\mathbf{y}}^M & \hat{\mathbf{z}}^M \end{bmatrix} = \begin{bmatrix} \frac{\hat{\mathbf{y}}^I \times \hat{\mathbf{z}}^M}{|\hat{\mathbf{y}}^I \times \hat{\mathbf{z}}^M|} & \frac{\hat{\mathbf{z}}^M \times \hat{\mathbf{x}}^M}{|\hat{\mathbf{z}}^M \times \hat{\mathbf{x}}^M|} & \hat{\mathbf{h}}_{\mathrm{D2/D1}} \end{bmatrix} \tag{4}$$

The angle of interest lies entirely in the mutual orbit plane. The out-of-plane components of these vectors can be specified by nulling out the bottom row of this rotation matrix and constructing a new mapping $R^{M/I}$.

$$\mathbf{R}^{M/I} = \begin{bmatrix} Q_{11} & Q_{12} & Q_{13} \\ Q_{21} & Q_{22} & Q_{23} \\ 0 & 0 & 0 \end{bmatrix} \tag{5}$$

The in-plane impact angle is then computed as the angle between the projected instantaneous velocities of DART and Didymos-B with respect to Didymos-A. For the baseline trajectory, this

angle must have a value between 175° and 180°.

$$\phi_{\mathrm{IP}} = \cos^{-1}\left(\mathbf{R}^{M/I}\,\hat{\mathbf{v}}^{I}_{\mathrm{sc/D1}} \cdot \mathbf{R}^{M/I}\,\hat{\mathbf{v}}^{I}_{\mathrm{D2/D1}}\right) \tag{6}$$

III. Baseline Trajectory Analysis

The trajectory optimization was conducted using two independent software tools. The first tool was the Evolutionary Mission Trajectory Generator (EMTG) tool, developed by NASA Goddard Space Flight Center [10, 11]. EMTG's monotonic basin hopping [12] feature allows convergence despite the presence of local minima, improving the search for a global minimum. The second tool is an in-house APL development, the Low-thrust INterplanetary eXplorer (LInX), which uses a Sims-Flanagan approach [13, 14]. The main aspect of this study was to verify that these two independent toolsets generated nearly identical trajectories. Doing so gives confidence that the baseline trajectory is both dynamically valid and achieves optimal performance.

The baseline heliocentric transfer trajectory is optimized to deliver the maximum spacecraft final mass. This objective effectively minimizes thruster and propellant use. The Earth escape date for this case comes from the mission development program and is set to October 3, 2021. The resulting baseline Heliocentric transfer, Fig. 2 and 3, has a thrust-coast-thrust structure. Although this control structure is similar to what is usually observed in rendezvous cases, this trajectory has a flyby-type final condition (position matching only). The two thrust arcs are near to the line of nodes between Earth and Didymos, such that inclination is optimally changed. In addition to adjusting inclination, the first thrust arc targets the mid-course flyby.

The two toolsets give excellent agreement. There is some variation in the amount of thrusting between the two arcs, but they result in nearly identical final mass values (within tenths of a kilogram), arrival dates (± an orbit period), and arrival constraints. As discussed in the missed thrust analysis below, the ability to adjust the orbit efficiently in two locations translates into missed thrust robustness within the trajectory. That is, the non-uniqueness of the thrusting time-histories, while providing the same final arrival conditions, is a benefit to the mission. The resulting trajectory, with representative margins, is given in Table 2.

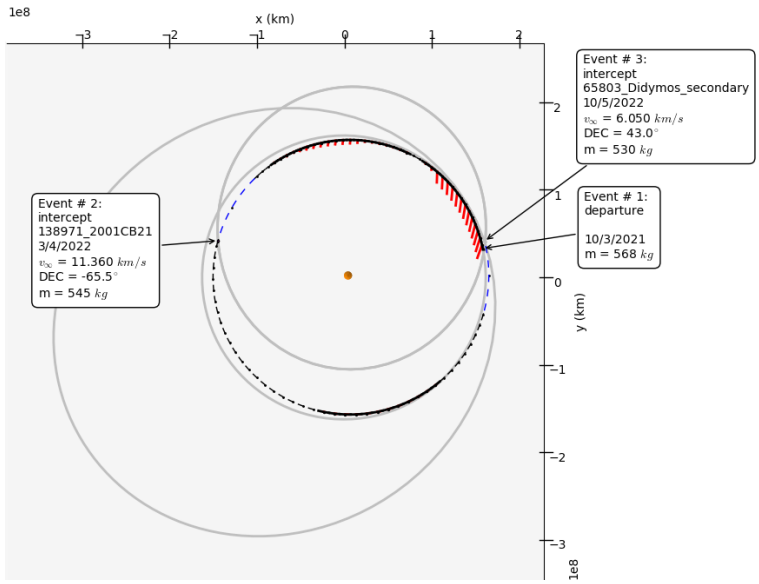

Fig. 2 The DART baseline heliocentric transfer trajectory in inertial frame.

Table 2 DART spacecraft mass allocation

Component		[kg]
DART Maximum Expected Dry Mass		483.0
Hydrazine with Margins		27.0
Neutral Mass		510.0
Deterministic Xenon Propellant		116.0
Operational Xenon Margin	3.0% det.	3.5
Missed Thrust Xenon Margin	5.0% det.	5.5
Xenon Residuals		3.0
Total Xenon		128.0
Unallocated Mass Margin		10.0
Delivered Mass		530.0
Total Wet Mass		648.0

A. Earth Gravity Assist

The EMTG searches included potential Earth Gravity Assists (EGA). These were speculated to offer a means of reducing the fuel consumption further. The heliocentric DART trajectory remains in an Earth-like orbit, so the short distances suggested that EGAs could be added. During the EGA, Earth's gravity would give an effective propellant-free Δv.

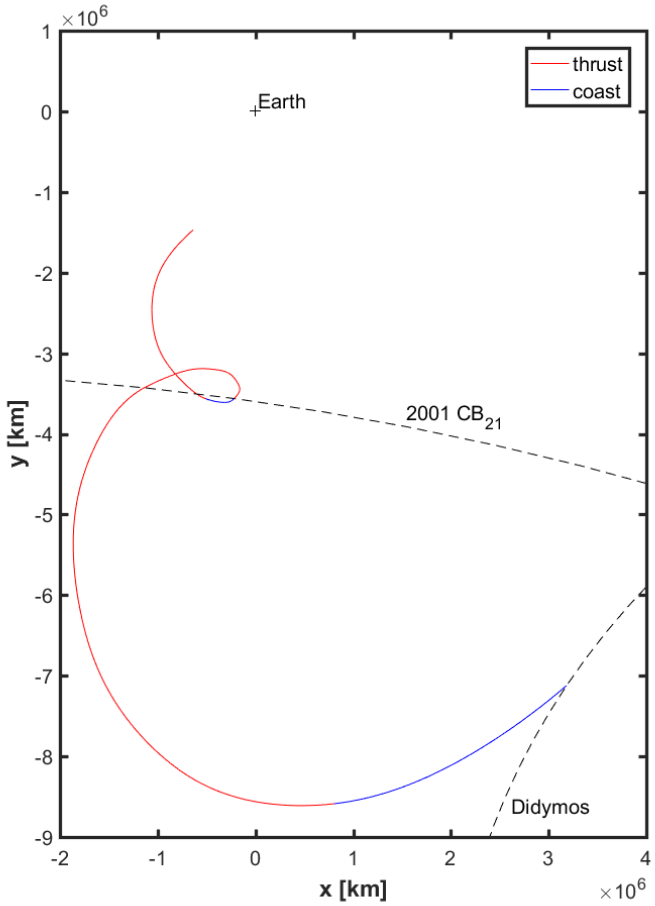

Fig. 3 The DART baseline heliocentric transfer trajectory in Sun-Earth rotating frame.

The search concluded that the EGA is not beneficial. In fact, the optimal solution, given in Fig. 4 requires roughly 5.5 kg more propellant than the baseline trajectory.

IV. Additional Mission Objectives and Trade Study

The baseline trajectory is designed to be fuel optimal (for a given escape state), which is important but not the only objective of interest to the mission. For example, the range of launch dates is a meaningful driver for mission schedule. In this section, we present the optimization results for additional objectives. Here, we consider optimality defined by the latest possible escape date, the shortest time-of-flight, and the maximum impact energy. These optimizations give context for the mission by defining the range of possible metrics. In these cases, the available propellant mass is constrained rather than minimized. The value is set to use no more than the baseline propellant

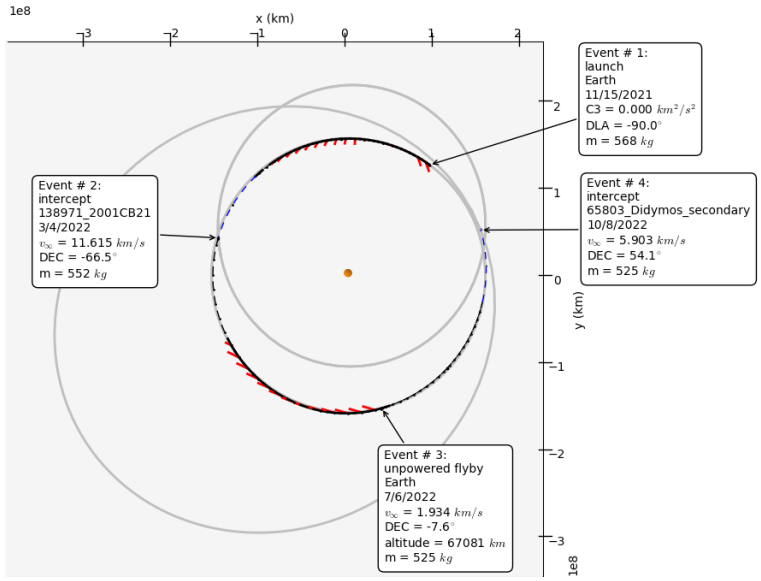

Fig. 4 The optimal DART transfer when an Earth gravity assist is included.

mass and its associated margin, such that the same spacecraft design can achieve these additional metrics. As in the baseline, all of the key constraints for launch and arrival must be satisfied for a valid solution.

A. Late Escape

DART is an interplanetary ride-share with a yet-to-be determined commercial launch vehicle. Launch delays are not uncommon so it is relevant to understand the schedule limits at which the mission can be conducted. Maximization of the launch escape date equates to enlarging the available dates for an interplanetary ride-share opportunity, yielding a major reduction of risk for the mission. For this trajectory, there is no dynamical penalty to launching early, since the spacecraft can coast in its Earth-like orbit indefinitely. Rather, the earliest launch date is driven by schedule constraints for delivery of the flight system. The latest launch date is a driver, as the October 2022 conjunction cannot be adjusted. This trajectory analysis studies the latest possible escape date that generates a feasible trajectory. Figure 5 shows the resulting trajectory. It is possible to delay escaping by 73 days to Dec. 16, 2021 and still complete the mission delivering 530 kg with a similar thrust structure.

This analysis for late escape does not necessarily imply that any launch spiral can connect to

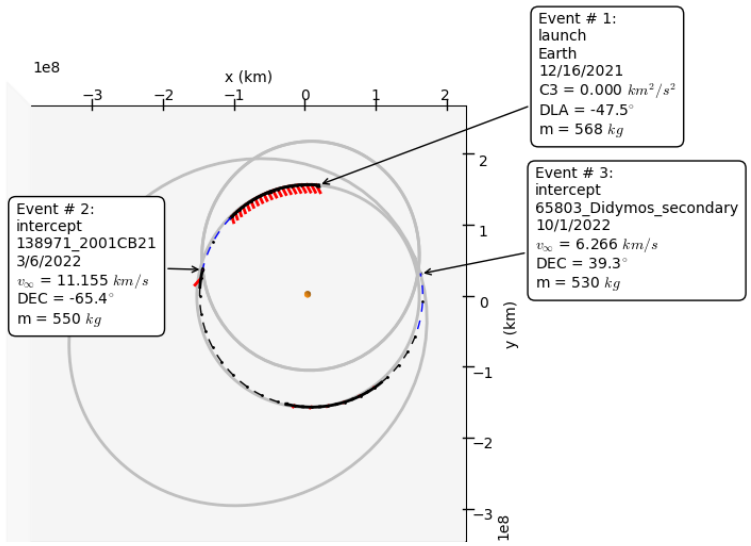

Fig. 5 The DART trajectory that escapes Earth as late as possible.

it. Rather, it is an epoch upper bound on when trajectory availability is reached. Future work will be dedicated to determining the latest feasible launch date for an arbitrary GTO.

B. Minimum Time-of-Flight

Here, we consider an objective that minimizes the duration of the Heliocentric Transfer phase. This metric helps to understand the minimum mission life of the spacecraft, which relates to design margins and operations costs. In this approach, we remove the constraints on the escape and the impact date, so that they can vary freely. Figure 6 shows that the result is nearly identical to the results of the objective for the latest escape date. That is, the transfer duration can be reduced by roughly 2.5 months, but this is entirely captured by escaping Earth later.

C. Maximum Kinetic Energy

Since the intent of the mission is to demonstrate a kinetic impact for planetary defense, a useful objective is the delivered kinetic energy ($E = \frac{1}{2}mv^2_{\mathrm{sc/D2}}$). This solution maximizes this kinetic energy subject to the available constraints. The solution, Fig. 7, launches 10 days after the baseline and arrives with 11.03 GJ of kinetic energy. This value exceeds the 9.69 GJ delivered in the baseline trajectory. The gain of 1.33 GJ is not trivial, but does not necessarily justify altering the available mission timeline. That is, this result indicates that the baseline has reasonable performance with

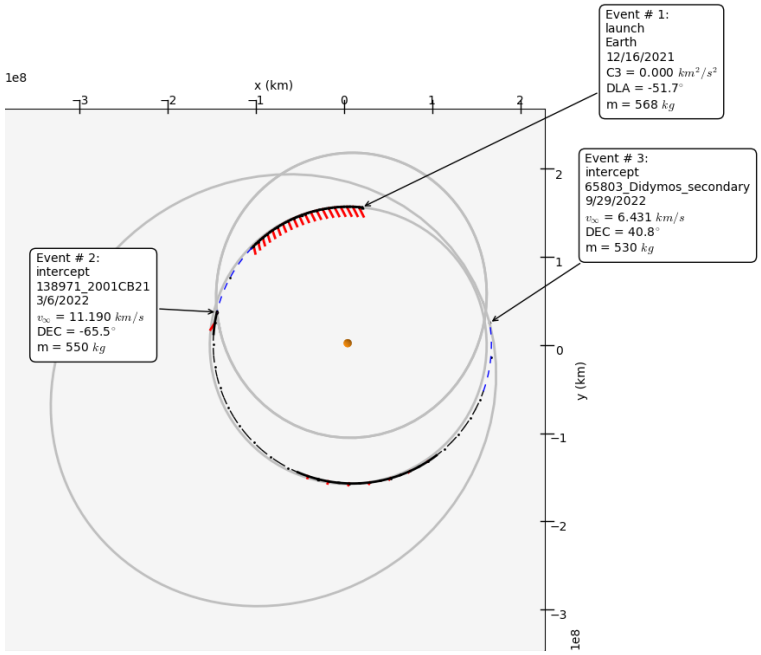

Fig. 6 The DART trajectory that minimizes time-of-flight.

respect to the maximum possible delivered energy metric.

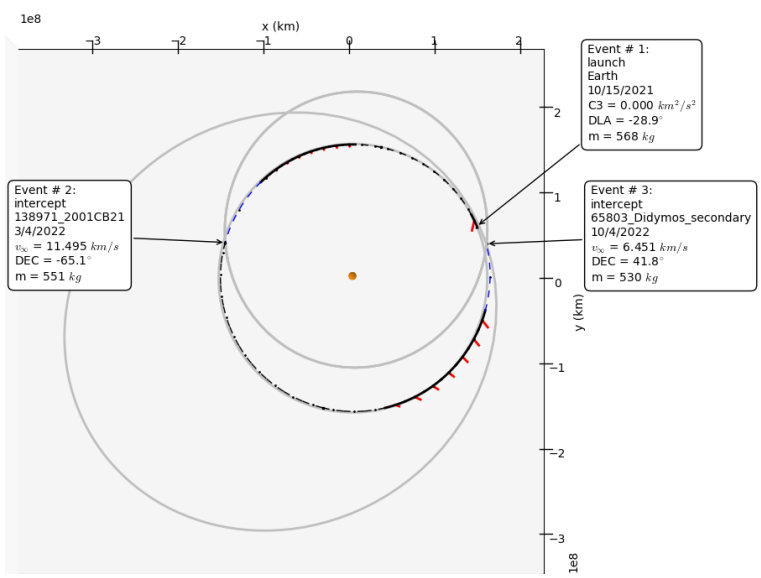

Fig. 7 The DART trajectory with maximum kinetic energy at impact.

D. Summary of Additional Objectives

Table 3 presents a summarized comparison of the above solutions against the baseline. Column 1 shows the case, column 2 the baseline value with respect to the metric, column 3 the comparison

case result, and column 4 the gain of the new solution compared with the baseline.

Table 3 Baseline Interplanetary Trajectory Performance

Case	Baseline Value	Optimal	Gain
Latest escape date	2021-Oct-03	2021-Dec-16	73 days
Minimum time of flight	368 days	288 days	80 days
Maximum kinetic energy	9.69 GJ	11.03 GJ	1.33 GJ

V. Missed Thrust Analysis

Given the baseline transfer trajectory, a second analysis is performed to evaluate the robustness against missed thrust events. Previous research [16] have suggested that this type of margin is most relevant to an operational mission. A missed thrust event is a case where the spacecraft is unable to operate its electric thruster. This can occur if the spacecraft enters a safe-mode due to an anomaly. While the anomaly is being resolved, the spacecraft is unable to deliver any thrust, and is thus coasting. When the spacecraft regains operation, it will no longer be on its original optimal trajectory, and a recovery trajectory must be designed. For some durations of missed thrust, no such recovery trajectory exists. This missed thrust analysis seeks to determine the maximum missed thrust duration, at any time in the Heliocentric transfer, for which the mission can still be executed.

Missed thrust events are not planned for and represent a critical risk. To that end, we assess the ability of the spacecraft to recover subject to reduced mission objectives. For example, the midcourse asteroid flyby can be removed if necessary. The duty cycle is modeled as 95% in order to use all available margin. We also evaluate differing levels of propellant allocation and mission constraints. For the latter, we consider the case that the original goals of the mission cannot be achieved, and attempt to assess reduced goals. Specifically, we analyze three cases:

1. Achieve the original impact conditions identically (match the full state);
2. Achieve impact conditions that satisfy the mission constraints, but are not necessary equal to the baseline values; and
3. Achieve "relaxed" impact conditions that satisfy reduced mission constraints.

For all cases, the solutions are allowed to miss the nominal asteroid flyby, if doing so enables the

Didymos-B impact.

A. Analysis Approach

The baseline is divided into a set of points, each of which is evaluated as the start of a missed thrust event. For this analysis, we consider points spaced 14 days apart, starting from the escape date. This spacing is fine enough to derive the key parameters and trends, while being computationally feasible. Figure 8 shows these points as x's overlaid on the reference trajectory. For each point, an optimal trajectory is found with the objective of initially coasting as much as possible, subject to constraints. That is, the optimizer is solving for the maximum duration of missed thrust, from which the mission can be recovered, at each point in the transfer.

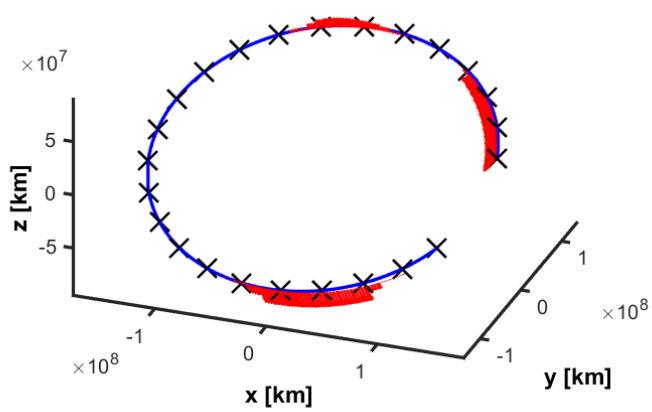

Fig. 8 The baseline DART trajectory with points indicating locations of missed thrust analysis.

In order to guide propellant margining at this phase of the mission design, different fuel margins are considered. A 0% fuel margin represents the final mass achieved in the baseline trajectory, 530 kg. Other values are given as percentages of the deterministic propellant value, 116 kg. These values correspond to: 0% (0.0 kg), 1% (1.2 kg), 3% (3.3 kg), 5% (5.8 kg) and 7% (8.1 kg). That is, this analysis presupposes that the mission has allocated differing amounts of propellant to the missed thrust recovery prior to launch. Each of these scenarios is assessed for the resulting duration of missed thrust robustness.

B. Results

The first case assesses the ability to recover the mission with the exact impact conditions. Figure 9 shows the results of this analysis, with a set of lines corresponding to different scenarios. Each line indicates the maximum recoverable duration of missed thrust (y-axis) that is initiated at a given time in the mission (x-axis). The bottom-most line gives the baseline trajectory's built-in robustness. That is, it indicates the current point and durations of coast times. During these times, if the spacecraft were unable to thrust, it would have no effect on the mission. The 0% line shows the duration that can be achieved without sacrificing propellant. That is, the 0% solution shows that the spacecraft can thrust differently early in the mission and achieve the same final conditions, especially since the duty cycle is increased to 95% and the asteroid flyby is no longer mandatory. For both of these optimal cases, there is a critical point at roughly 275 days where the spacecraft must thrust in order to satisfy the constraints. This is a point where any missed thrust event would end the mission, if no propellant were available. However, the 1% line shows that a modest amount of propellant is able to give over 14 days of robustness at this critical point. As additional margin is allocated, there are diminishing returns. In fact, the 5% and 7% lines are nearly indistinguishable for most of the mission.

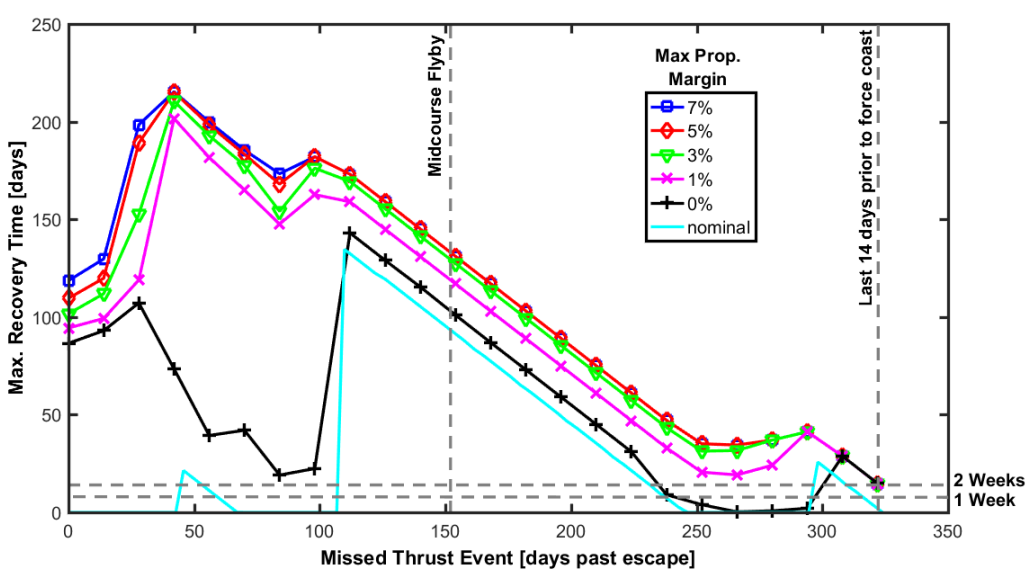

Fig. 9 Results for the missed thrust analysis with fixed impact conditions.

The second case assesses the ability of the mission to recover while still satisfying the baseline mission constraints. That is, the arrival state can vary, but is still subject to the same constraints. This offers an improvement in that it is less restrictive. The third case further improves the feasibility of recovery by reducing some of the arrival constraints. Specifically, the maximum solar phase angle is a driving constraint for the baseline trajectory. The standard and "relaxed" constraints are given in Table 4.

The results of these two cases are presented in Fig. 10, which uses solid lines to indicate the results of the standard constraints and dashed lines to indicate the results of the relaxed constraints. The relaxed constraint case shows a clear benefit near the end of the mission in that the 0% case is recoverable with 14 days of missed thrust. The relaxation of the solar phase constraint enables the trajectory to recover without using additional mass.

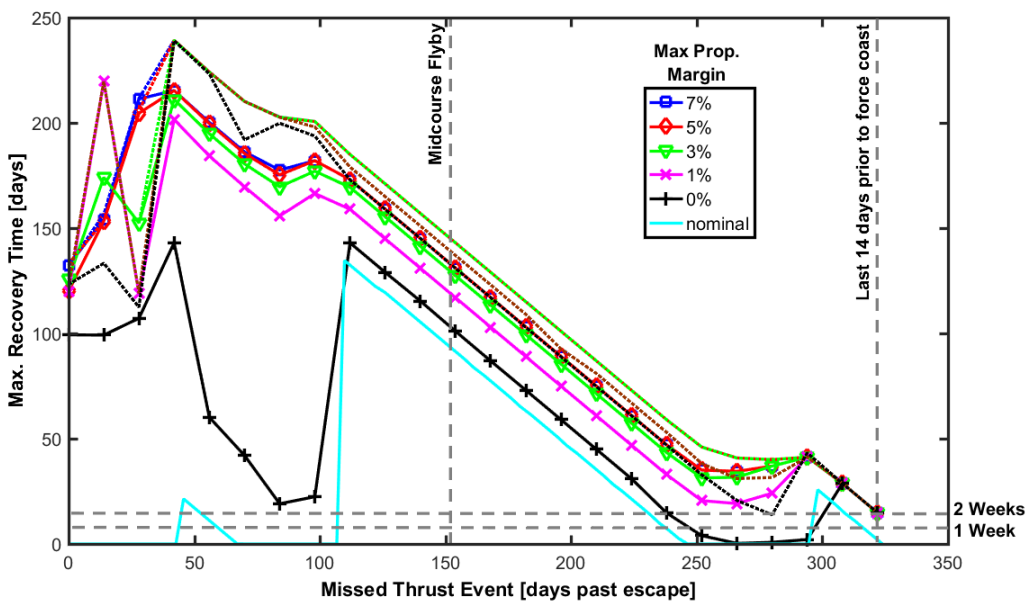

Fig. 10 Results for the missed thrust analysis with standard and relaxed impact constraints (the solid line indicates results for standard constraints and the dotted line indicates results for relaxed constraints).

The results follow one's intuition, in that each reduction of the constraints results in a higher recoverable missed thrust duration. Likewise additional margin always meets or exceeds the lower margin cases. The relative improvement between the cases is given in Figs. 11 and 12, which show

the difference in recoverable missed thrust between the pairs of cases.

Given these results, the mission is allocating a propellant margin of 5%, which ensures a 14-day period of recoverable missed thrust duration at any point in the mission for any scenario. This analysis indicates that this desired robustness can also be achieved by varying the arrival constraints, so a 5% allocation is conservative.

Table 4 Constraint Scenarios used in the Missed Thrust Analysis

	Max. solar Phase Angle	Out-of-Plane Impact Angle	In-Plane Impact Angle
Standard Constraints	60°	±30°	$175° \leq \phi_{IP} \leq 180°$
Relaxed Constraints	75°	±32.5°	$170° \leq \phi_{IP} \leq 180°$

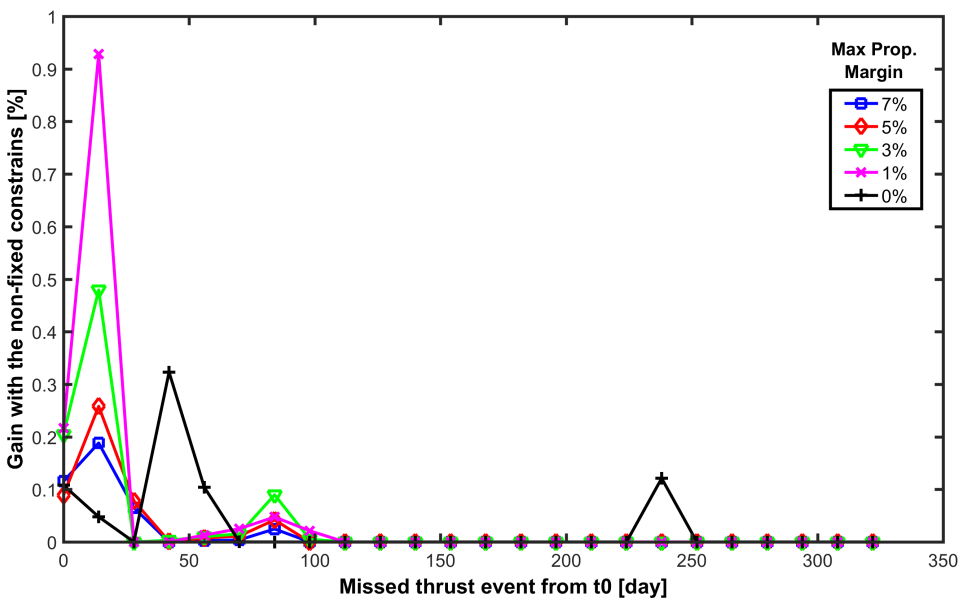

Fig. 11 Relative improvement of the standard constraints over the fixed impact state constraint in the missed thrust analyses.

VI. Contingency Trajectories

It was shown in the previous section that the baseline is robust to missed thrust. However, there are still cases where the spacecraft may be unable to achieve its nominal impact with Didymos-B.

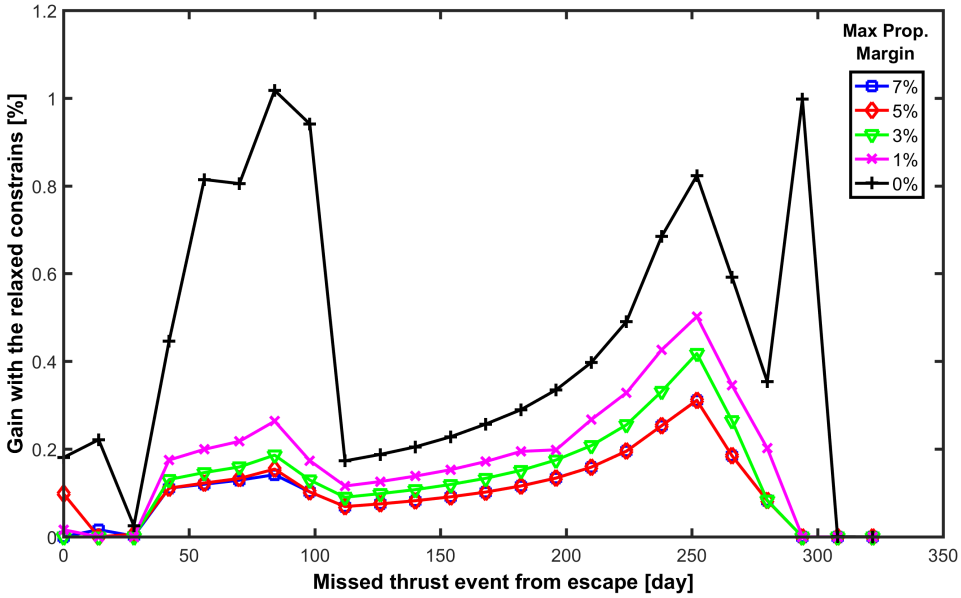

Fig. 12 Relative improvement of the relaxed constraints over the standard constraints in the missed thrust analyses.

For example, the missed thrust analysis indicates that after 238 days, the spacecraft cannot tolerate a missed thrust event lasting longer than 14 days. Although that is a large duration, there is no guarantee that an anomaly may be identified and corrected in time. Likewise, any spacecraft anomaly during the final weeks or hours of the mission may result in a missed impact. These cases, though unlikely, motivate the following analysis, which considers an impact of Didymos-B approximately 2 years after the nominal impact date. These contingency trajectories represent final efforts to recover the mission, despite some critical failure, and are not design points.

A. Critical Missed Thrust

The first scenario targets an impact solution following a missed thrust exceeding 14 days, located 238 days after escape. The above missed thrust analysis showed that the spacecraft is unable to recover from this duration. Here, we consider the option of recovering the mission by targeting an impact at an unconstrained later date. The duty-cycle is set to 90% and the optimization objective is defined to minimize propellant mass.

The results, given in Fig. 13 show that the mission can reach the target in 2024 at Didymos's

next perihelion passage. During this time, DART completes two heliocentric orbits. The thruster uses roughly 3.3 kg, or 3% of the deterministic propellant loading. This amount is within the allocated missed thrust mass budget, so it would represent a feasible option with no changes to the spacecraft design. The impact satisfies all of the mission trajectory requirements. As considered for the baseline, we also considered the use of an Earth gravity assist to decrease the propellant consumption. Again, the EGA offers no benefit. The search tool identified an optimal solution that used 16.26% of the deterministic propellant, significantly worse than the non-EGA solution above.

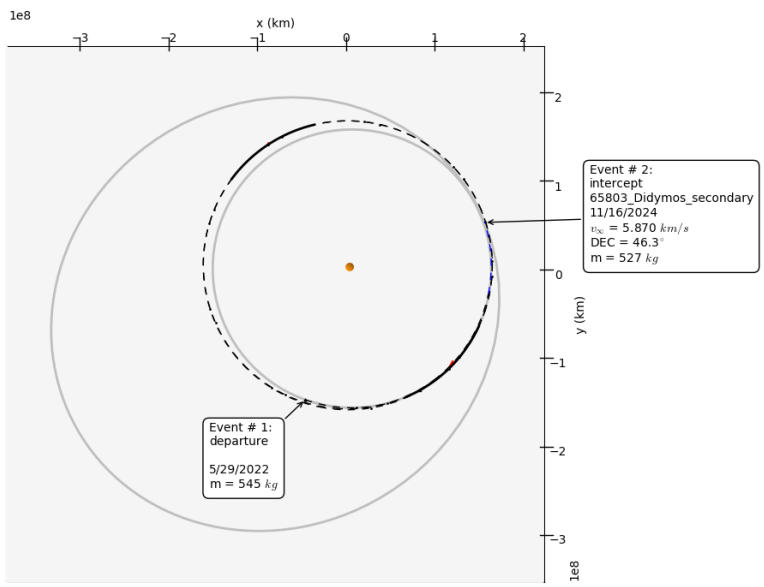

Fig. 13 The DART second impact contingency trajectory for a missed thrust during the critical period.

B. Missed Impact

Here, we consider the case where the spacecraft reaches the Didymos system nominally, but fails to impact Didymos-B. The trajectory design begins at the final state of the baseline and targets a second impact opportunity in 2024. This direct re-targeting results in a final spacecraft mass well below the allocated margins, requiring more propellant than is reasonable to allocate. This solution is given in Fig. 14. This analysis indicates that, as formulated, the mission cannot recover from a missed impact on the baseline trajectory.

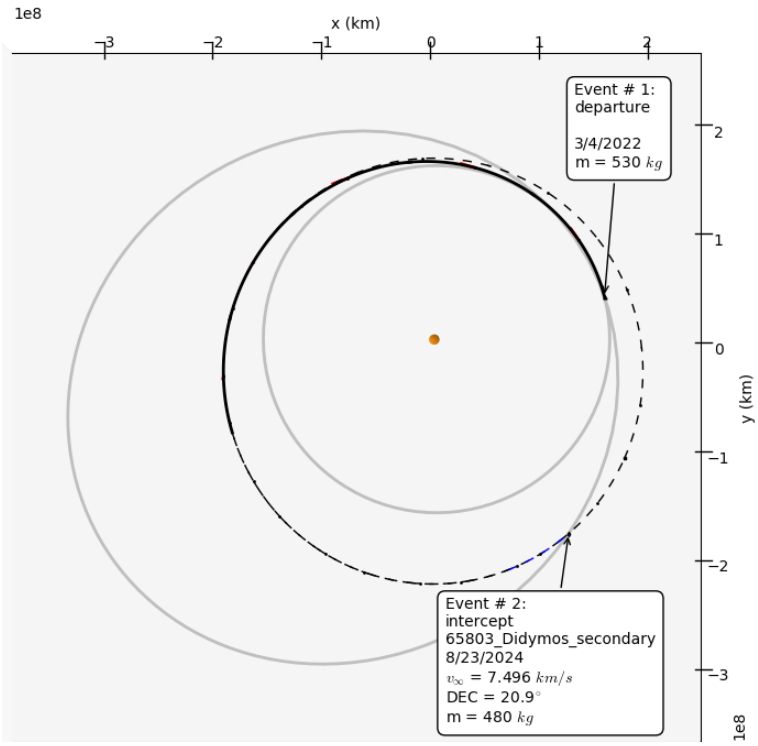

Fig. 14 The DART second impact contingency trajectory for an unsuccessful initial impact attempt.

C. Resonant Return

Although a direct re-targeting from the baseline trajectory is not feasible, the former missed thrust case suggests that a second impact can be enabled by adjusting the baseline trajectory. Here we redesign the reference trajectory to explicitly enable a second impact opportunity. In this case, the new baseline still includes the midcourse flyby of 2001 CB_{21}. Following the nominal impact date in October of 2022, the spacecraft completes two heliocentric orbits and re-encounters Didymos in 2024. For each impact opportunity all of the arrival constraints are satisfied.

The solution is presented in Fig. 15 and requires roughly 3.3 kg of additional propellant, which is within 3% of the previous baseline trajectory's deterministic propellant loading. Again, this suggests that the spacecraft would not necessarily need to be redesigned, though its available propellant margin would be reduced. In the new solution, the spacecraft achieves a resonant trajectory with Didymos after the fist encounter, resulting in a nearly ballistic Didymos-to-Didymos transfer.

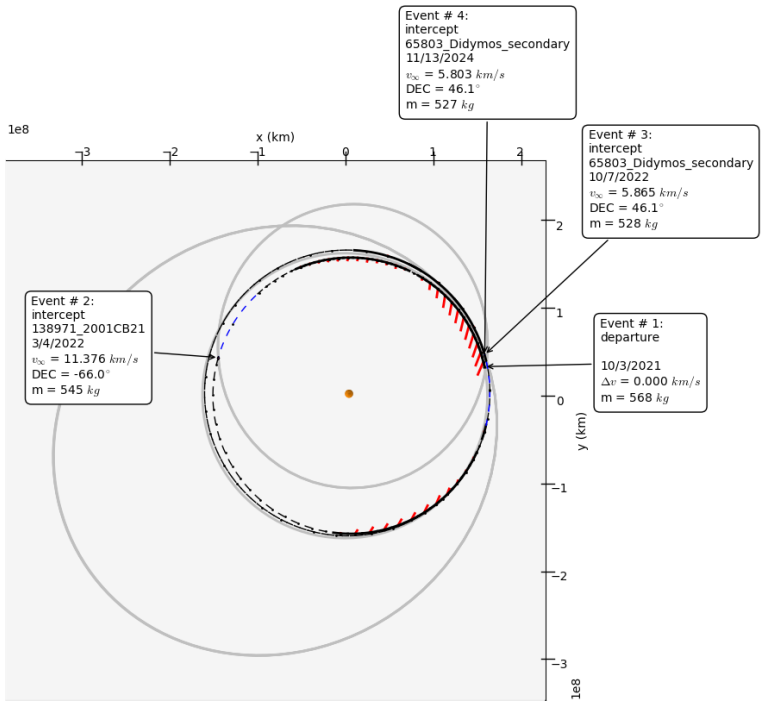

Fig. 15 The mass optimal DART trajectory designed with two impact opportunities (resonant return).

VII. Conclusions

The NASA Double Asteroid Redirection Test will be the first mission to test the kinetic impactor concept for planetary defense. The mission targets the impact of the secondary member of the (65803) Didymos binary system. The Heliocentric transfer was designed using an optimization tool that includes the mission constraints for a maximum final spacecraft mass. The span of possible mission objectives was explored, suggesting an available launch period of at least 2.5 months after the baseline case and up to 14% higher impact energy. The trajectory was assessed for robustness to missed thrust events. As margined, the spacecraft can recover from any missed thrust event in the mission shorter than 14 days. For most of the trajectory, the mission can recover from many weeks of missed thrust, but the critical period occurs near to impact. The analysis suggests that if needed, one can trade propellant margin for mission constraints, arriving with poorer lighting conditions or suboptimal geometry. During the critical missed thrust period, if an event exceeds 14 days, it is possible to target a second impact opportunity in 2024 as a final means of attempting to recover the mission. This led us to develop an alternate transfer trajectory wherein a second impact

was explicitly targeted. Doing so requires approximately 3 kg more propellant, which is modest compared to the overall mission budget.

VIII. Acknowledgments

This research was conducted with support from NASA's Planetary Defense Coordination Office.

[1] O.P. Popova et al., Chelyabinsk Airburst, Damage Assessment, Meteorite Recovery, and Characterization, Science, Vol. 342, Issue 6162, pp. 1069-1073, November (2013). DOI: 10.1126/science.1242642

[2] R.P. Turco and O.B. Toon and C. Park and R.C. Whitten and J.B. Pollack and P. Noerdlinger, An analysis of the physical, chemical, optical, and historical impacts of the 1908 Tunguska meteor fall, Icarus, Volume 50, Issue 1, Pages 1-52 (1982). ISSN: 0019-1035 DOI: 10.1016/0019-1035(82)90096-3.

[3] Committee to Review Near-Earth Object Surveys and Hazard Mitigation Strategies Space Studies Board, Defending Planet Earth: Near-Earth Object Surveys and Hazard Mitigation Strategies, National Research Council, pages 152 (2010). ISBN: 978-0-309-14968-6, DOI: 10.17226/12842.

[4] A.F. Cheng and J. Atchison and B. Kantsiper and A.S. Rivkin and A. Stickle and C. Reed and A. Galvez and I. Carnelli and P. Michel and S. Ulamec, Asteroid Impact and Deflection Assessment Mission, Acta Astronautica, Vol. 115, pages 262 - 269 (2015). ISSN: 0094-5765, DOI: 10.1016/j.actaastro.2015.05.021.

[5] J. Atchison and M. Ozimek and B. Kantsiper and A.F. Cheng, Trajectory Options for the DART Mission, 66th International Astronautical Congress, IAC-15-C1.1.31080, Jerusalem, Israel (2015).

[6] L.A.M. Benner and J. Margot and M.C. Nolan and J.D. Giorgini and M. Brozovic and D.J. Scheeres and C. Magri and S.J. Ostro, Radar Imaging and a Physical Model of Binary Asteroid 65803 Didymos, American Astronomical Society, Division for Planetary Sciences Meeting Abstracts, Bulletin of the American Astronomical Society, Vol. 42, page 1056, id 13.17, October (2010).

[7] N.M. Gaftonyuk and Y.N. Krugly and I.E. Molotov, Results of Photometric Observations of Potentially Hazardous Asteroids, Small Bodies of the Solar System, The Asteroid-Comet Hazard Conference Proceedings, pages 49 - 51 (2009).

[8] J. Van Noord and D. Herman, Application of the NEXT Ion Thruster Lifetime Assessment to Thruster Throttling Strategies, AIAA-2008-4526, 44th AIAA/ASME/SAE/ASEE Joint Propulsion Conference and Exhibit, Hartford, CT, July (2008).

[9] Jeffrey M. Woytach and Michael J. Patterson and George C. Soulas and Michael V. Aulisio and Rohit Shastry, NASAâĂŹs Evolutionary Xenon Thruster - Commercial (NEXT-C): Throttle Table Baseline, GRC-NEXTC-DOC-041, NASA John H. Glenn Research Center, Cleveland, Ohio, January (2017).

[10] J.A. Englander and B.A. Conway, An Automated Solution of the Low-Thrust Interplanetary Trajectory Problem, Journal of Guidance, Control, and Dynamics, AIAA (2016). [Accepted]

[11] J.A. Englander and J.M. Knittel and K. Williams and D. Stanbridge and and E.H. Donald, Validation of a Low-Thrust Mission Design Tool Using Operational Navigation, 27th AAS/AIAA Space-Flight Mechanics Meeting, AAS Paper 17-204, San Antonio, Texas, February (2017).

[12] J.A. Englander and A.C. Englander, Tuning Monotonic Basin Hopping: Improving the Efficiency of Stochastic Search as Applied to Low-Thrust Trajectory Optimization, 24th International Symposium on Space Flight Dynamics, Laurel, MD, May (2014).

[13] J.A. Sims and S.N. Flanagan, Preliminary Design of Low-Thrust Interplanetary Missions, AAS/AIAA Astrodynamics Specialist Conference, AAS Paper 99-338, Girdwood, Alaska, August (1999).

[14] M.T. Ozimek and J.A. Atchison, NASA Double Asteroid Redirection Test (DART) Low-Thrust Trajectory Concept, 27th AAS/AIAA Space-Flight Mechanics Meeting, AAS Paper 17-221, San Antonio, Texas, January (2017).

[15] B.K. Kantsiper, The Double Asteroid Redirection Test (DART) Mission Electric Propulsion Trade, IEEE Aerospace Conference, Paper 2.1213, Big Sky, Montana, March (2017).

[16] D.Y. Oh and D. Landau and T. Tandolph and P. Timmerman and J. Chase and J. Sims and T. Kowalkowski, Analysis of System Margins on Deep Space Missions Utilizing Solar Electric Propulsion, AIAA 2008-5286, AIAA Joint Propulsion Conference, Hartford, Connecticut, July (2008).

[17] B.J. Zimmerman and B. Wie, A GPU-accelerated multiphase computational tool for asteroid fragmentation/pulverization simulation. 26th AAS/AIAA Space-Flight Mechanics Meeting, AAS Paper 16-242, Napa, California, February (2016).